

# Variable property effects in the analysis of a stagnation point diffusion flame

I. M. KENNEDY

Aeronautical Research Laboratories, PO Box 4331 GPO, Melbourne, Australia

(Received 15 February 1985 and in final form 4 June 1985)

**Abstract**—The effect of variations in fluid properties on the analysis of a stagnation point diffusion flame has been studied by means of a numerical calculation. The thermochemistry of the flame was prescribed by an empirical correlation of species concentrations and temperature with a conserved scalar (the fuel atom mass fraction). In this way the mixing process in the diffusion flame was decoupled from the chemical kinetics. Variations in the Schmidt number for the mixture fraction did not have a significant effect on the numerical prediction of the atom mass fraction profile in the flame. However, the assumption of a constant value for  $\rho\mu$  through the methane–air flame caused a significant overprediction of the mixing-layer thickness. An average value of  $\rho\mu$  through the boundary layer yielded satisfactory predictions of the mass fraction profile.

## INTRODUCTION

LAMINAR boundary-layer flows which involve the mixing of different gases or which support exothermic chemical reactions can exhibit substantial variations in fluid properties such as density, viscosity and thermal and mass diffusivities. Prediction of these flows must either incorporate detailed variations in properties or resort to an empirical constant-property scheme. Calculation methods in the latter category commonly employ an approach in which fluid properties are evaluated at a reference composition or temperature [1].

A number of different constant-property schemes have been applied to mixing flows. Knuth [2] used a reference composition to correlate data for an isothermal boundary layer of air into which helium was injected. Property variations which arise from droplet vapourization or combustion have been accounted for by the use of reference temperatures [3, 4].

The successful application of a constant property approach usually involves a judicious and *ad hoc* choice of reference conditions. Failure to account for variations in properties, however, can lead to erroneous and unacceptable results [5]. Most analytical treatments of boundary-layer combustion adopt this course as a result of the simplifications which it affords.

Theoretical analyses of chemically reacting boundary layers yield a term  $\rho\mu$  in the momentum equation and a Schmidt number,  $\nu/\mathcal{D}$ , in each species conservation equation [6]. Because density is proportional to  $T^{-1}$  and viscosity is approximately proportional to  $T^{1.5}$  it is commonly argued that the product,  $\rho\mu$ , can be assumed to be constant across the boundary layer. Similarly, the Schmidt number is often assumed to be constant, usually with a value of 1. Because of the simplifications which they afford, these assumptions are routinely applied in calculations of reacting boundary-layer flows [7–10]. However, in

some cases the change in composition across a flame can cause significant variations in properties. For example,  $\rho\mu$  for methane at 300 K is  $7.2 \times 10^{-6} \text{ kg}^2 \text{ m}^{-4} \text{ s}^{-1}$  and for air at 300 K it is  $2.1 \times 10^{-5} \text{ kg}^2 \text{ m}^{-4} \text{ s}^{-1}$ , a factor of 3 difference.

Some studies of laminar reacting boundary-layer flows have addressed the role of variable fluid properties. Marathe and Jain [11] analysed a counter-flow diffusion flame with variable Prandtl and Schmidt numbers. They found that the position of the flame depended on the Schmidt number and that the maximum flame temperature was affected by the Lewis number. However, their analysis relied upon the assumption of constant  $\rho\mu$ . In a numerical calculation of a methane–air stagnation point diffusion flame with one-step kinetics Takeno [12] assumed unit Prandtl and Lewis numbers and a constant value of  $\rho\mu$ . He concluded that the latter assumption probably accounted for the overprediction of the boundary-layer thickness by about 37%. More recently, Ishizuka and Tsuji [13] analysed the same diffusion flame primarily to ascertain the influence of variable Lewis numbers on flame temperature. In their analysis they used a flame sheet combustion model with constant fluid density, viscosity and thermal conductivity. As a result their analysis was not likely to represent the boundary-layer structure accurately although they found an appreciable effect of Lewis number on flame temperature for some conditions.

Property variations are fully accounted for in detailed numerical calculations of flames [14, 15] which include complex chemical kinetics. However, there is strong coupling between the exothermic, high activation energy reactions in flames and transport properties which are dependent on temperature and composition. As a result it is not possible to examine by these detailed calculations the isolated effect of constant property assumptions in analytical models of reacting boundary-layer flows.

## NOMENCLATURE

|  |  |
|--|--|
| $a$ velocity gradient [ $\text{s}^{-1}$ ]                | $\nu$ kinematic viscosity [ $\text{m}^2 \text{s}^{-1}$ ] |
| $\mathcal{D}$ diffusivity [ $\text{m}^2 \text{s}^{-1}$ ] | $\xi$ mixture fraction                                   |
| $f$ stream function                                      | $\rho$ density [ $\text{kg m}^{-3}$ ].                   |
| $H$ enthalpy [J]   |  |
| $M$ number of chemical species                           |  |
| $p$ pressure [ $\text{N m}^{-2}$ ]                       | Subscripts   |
| $R$ burner radius [m]                                    | C with respect to carbon atoms                           |
| $Sc$ Schmidt number                                      | e at the edge of mixing layer                            |
| $T$ temperature [K]                                      | $i$ for species $i$                                      |
| $u$ tangential velocity component [ $\text{m s}^{-1}$ ]  | N with respect to nitrogen atoms                         |
| $v$ normal velocity component [ $\text{m s}^{-1}$ ]      | O with respect to oxygen atoms                           |
| $X$ mole fraction  | W at burner surface                                      |
| $x$ tangential coordinate [m]                            | 1 in feed-stream 1                                       |
| $Y$ mass fraction  | 2 in feed-stream 2                                       |
| $y$ normal coordinate [m].                               | $\infty$ in the free stream.                             |
| Greek symbols  |  |
| $\eta$ non-dimensional normal coordinate                 | Superscripts   |
| $\mu$ dynamic viscosity [ $\text{Ns m}^{-2}$ ]           | denotes differentiation with respect to $\eta$ .         |

The approach which is adopted in this study decouples the fluid mechanics and chemistry. On the basis of experimental evidence, the thermochemistry of a diffusion flame is taken to depend only on the local stoichiometry or degree of mixing of the fuel, air and products. An empirical correlation of measured data with the degree of mixedness in the flame is used to establish the composition, temperature and hence properties such as  $\rho$ ,  $\mu$  and  $\mathcal{D}$  of the fluid. By this means the effect on the boundary-layer structure of realistic variations in fluid properties can be studied. The possible errors associated with the assumptions of constant  $\rho\mu$  and Schmidt number can then be investigated by attempting to reproduce the flame structure with a numerical calculation which incorporates either constant or variable transport properties.

## THE MIXTURE FRACTION

Experimental evidence from a variety of flame configurations suggests that temperature and composition can be correlated by a parameter which is a measure of the degree of mixedness of reactants. In his analysis of stagnation point diffusion flames Bilger [16] used the fuel atom mass fraction, also known as the mixture fraction, as the correlating parameter. Alternatively, Mitchell *et al.* [17] correlated composition and temperature in their flame with the local equivalence ratio. The mixture fraction has been adopted in the present study because of its greater conceptual clarity and the fact that it is bounded between 0 and 1 (the local equivalence ratio goes to infinity for pure fuel).

For a two-stream mixing flow the mixture fraction is defined as

$$\xi \equiv \frac{Y_i - Y_{i1}}{Y_{i2} - Y_{i1}} \quad (1)$$

where  $Y_{i1}$ , for example, is the mass fraction of element  $i$  in stream 1. Because  $\xi$  is defined in terms of element mass fractions it is conserved under chemical reaction, i.e. it is neither created nor destroyed by reaction. If the diffusivities of all species and the thermal diffusivity are equal then it can be shown that  $\xi$  is unique, regardless of which element is used to define it. These conditions are incorporated in the Shvab-Zeldovich formulation of the conservation equations [6].

Bilger [16] analysed the gas-sampling results of Tsuji and Yamaoka [18] for a methane-air laminar diffusion flame which was burning around a porous cylinder. He found that the use of data for the carbon element mass fraction gave the most satisfactory representation of  $\xi$  through the flame, particularly with regard to the stoichiometric value. Values of  $\xi$  which were derived from nitrogen or oxygen atom data did not yield the correct stoichiometric value of 0.055 at the flame. This discrepancy for nitrogen and oxygen atom data arose in part from errors in the determination of  $\xi$  which involved small differences in large quantities for these elements. The effect of different diffusivities for species containing oxygen and nitrogen atoms may also have contributed to the error in  $\xi_N$  and  $\xi_O$  at the flame front. Although it is possible to define in terms of carbon, hydrogen and oxygen element mass fractions a mixture fraction which yields the correct stoichiometric value regardless of diffusivities [19], the simpler definition

based on carbon element mass fraction has been used in this study.

The data of Abdel Khalik [20] for a heptane–air diffusion flame around a porous sphere was also analysed by Bilger [16]. He found that when measurements of stable species concentrations at different locations around the sphere were plotted as functions of  $\xi$  they collapsed onto one curve. The correlation of composition with  $\xi$  was not sensitive to the details of the flow field.

Figure 1 shows the concentrations of three major stable species plotted against the mixture fraction,  $\xi_c$ , which was derived from Tsuji and Yamaoka’s data for their methane–air flame [18]. The carbon atom mass fraction was used to evaluate  $\xi$ . Also shown in this figure are data derived in the same manner from the measurements of Mitchell *et al.* [17] in a laminar, methane–air flame on a tubular burner. The correlation of species concentrations with mixture fraction is similar in both cases. Less satisfactory, however, is the comparison between temperature measurements shown in Fig. 2. It should be noted that the thermocouple measurements by Mitchell *et al.* [17] were corrected for radiation and conduction whereas the measurements by Tsuji and Yamaoka [18] were not. This essentially accounts for the difference in the measured maximum flame temperatures although the lower strain rate in the experiment of Mitchell *et al.* [17] would also result in a slightly higher flame temperature. The presence of the porous burner in the experiments of

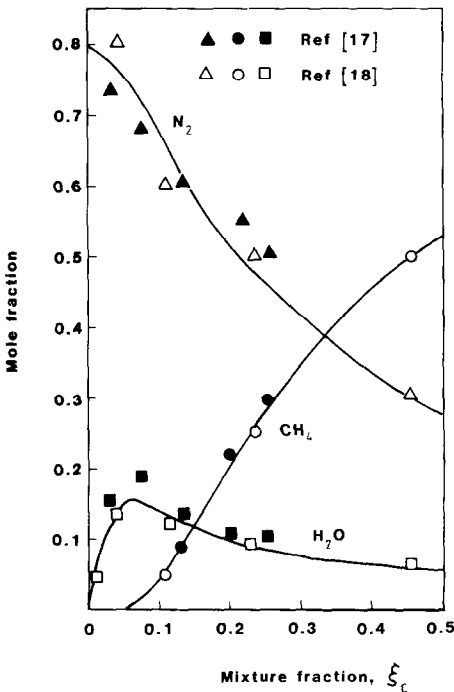


FIG. 1. Empirical correlations of species concentrations in methane–air diffusion flames with  $\xi$  (— correlation curve used in calculations).

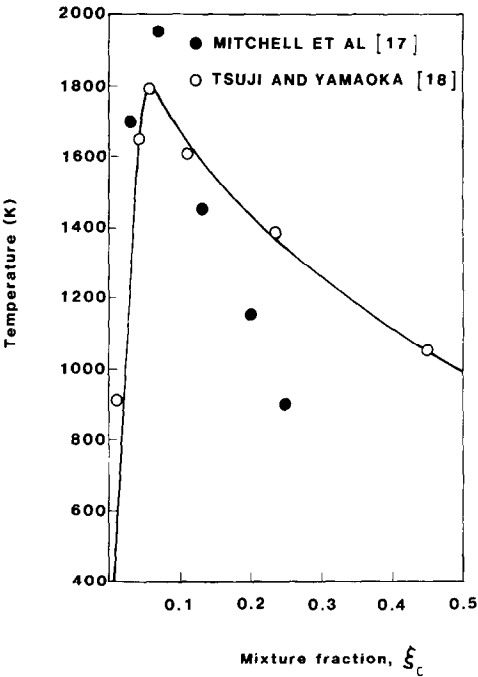


FIG. 2. Empirical correlations of temperature in methane–air diffusion flames with  $\xi$  (— correlation curve used in calculations).

Tsuji and Yamaoka [18] accounts for the difference between the two correlations on the fuel side of the flame.

VARIABLE PROPERTIES

Given the empirical correlation of  $\xi$  with species concentrations and temperature, it is possible to determine fluid density, viscosity and, less directly, multicomponent species diffusivities as functions of  $\xi$ . The latter quantities can be estimated from the kinetic theory for transport processes [21]. The data of Tsuji and Yamaoka for a methane–air diffusion flame [18] and a propane–air diffusion flame [22] have been analysed in this manner to yield profiles of transport properties through the flames.

The product  $\rho_e \mu_e / \rho \mu$  is shown in Fig. 3 for methane and propane data. In a methane flame this product varies between 1 (in the free stream) to about 3.2 near the porous burner. There is considerably less variation in the product of  $\rho_e \mu_e / \rho \mu$  in a propane flame. Although the viscosity of methane is about 50% greater than propane, its much lower density accounts for the large value of  $\rho_e \mu_e / \rho \mu$  at the burner. It is clear from Fig. 3 that the use of a value of unity for  $\rho_e \mu_e / \rho \mu$  cannot be justified, particularly for a methane diffusion flame.

Also shown in Fig. 3 is the profile of Schmidt number which was calculated for the methane flame of Tsuji and Yamaoka [18]. The diffusivity was taken to be the effective binary diffusivity of nitrogen in the mixture. This Schmidt number varies between 0.6 and 0.8 and

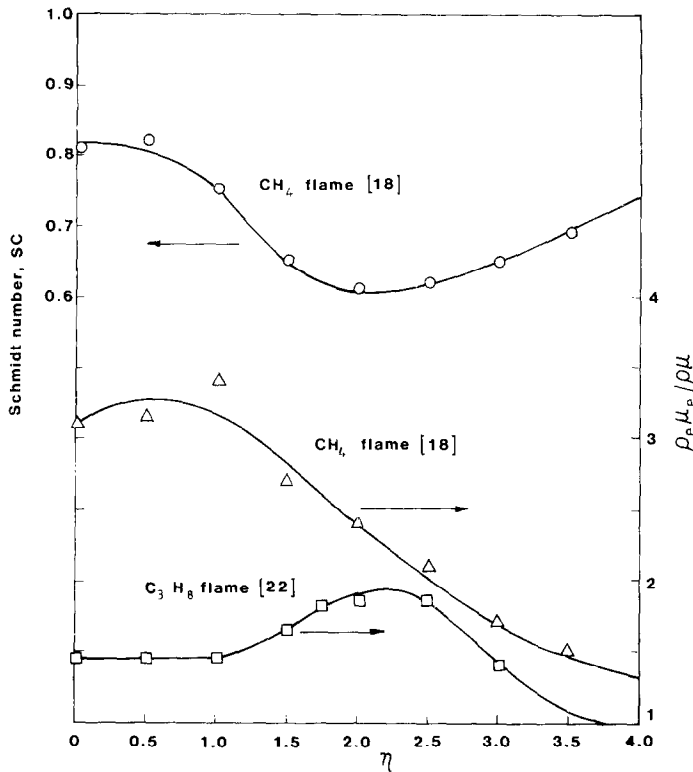


FIG. 3. Variation of properties through the methane-air diffusion flame [17] and propane-air diffusion flame [21] of Tsuji and Yamaoka.

has a value in the free stream of 0.75. Thus, the assumption of unit Schmidt numbers in the methane-air diffusion flame does not appear to be justified *a priori*.

STAGNATION POINT DIFFUSION FLAME

In order to make use of the detailed measurements of Tsuji and Yamaoka [18], calculations have been performed for the flow configuration which is shown in Fig. 4. Methane is ejected uniformly around the circumference of a porous cylinder. Air is blown across the cylinder at an up-stream velocity of  $v_\infty$ . Because of the stoichiometry of the methane-air reaction the diffusion flame is established on the air side of the stagnation point.

The momentum equation and the equation of conservation of mixture fraction can be written in boundary-layer form as

$$\rho u \frac{\partial u}{\partial x} + \rho v \frac{\partial u}{\partial y} = \frac{\partial}{\partial y} \left( \mu \frac{\partial u}{\partial y} \right) - \frac{dp}{dx} \tag{2}$$

$$\rho u \frac{\partial \xi}{\partial x} + \rho v \frac{\partial \xi}{\partial y} = \frac{\partial}{\partial y} \left( \rho \mathcal{D} \frac{\partial \xi}{\partial y} \right). \tag{3}$$

The two equations are coupled by the dependence of  $\rho$  and  $\mu$  on  $\xi$ .

The interpretation of the diffusivity which appears in equation (3) will be discussed later in this section.

The pressure gradient term in equation (2) can be written in an alternative form using the Bernoulli equation as

$$-\frac{dp}{dx} = \rho_e u_e \frac{du_e}{dx} \tag{4}$$

$$= \rho_e u_e a \tag{5}$$

in which  $a$  is the velocity gradient for potential flow at small  $x$  (close to the stagnation streamline)

$$a = 2v_\infty/R. \tag{6}$$

The normal coordinate is non-dimensionalized [23] as

$$\eta = \left( \frac{a}{v_e} \right)^{1/2} \int_0^y \rho/\rho_e dy^*. \tag{7}$$

The introduction of a non-dimensional stream function,  $f$ , satisfies the requirement of continuity so that the velocity components are

$$u = u_e f' \tag{8}$$

and

$$\rho v = -(a\rho_e\mu_e)^{1/2}f. \tag{9}$$

The prime denotes differentiation with respect to  $\eta$ . The momentum equation in terms of  $f$  and  $\eta$  in the

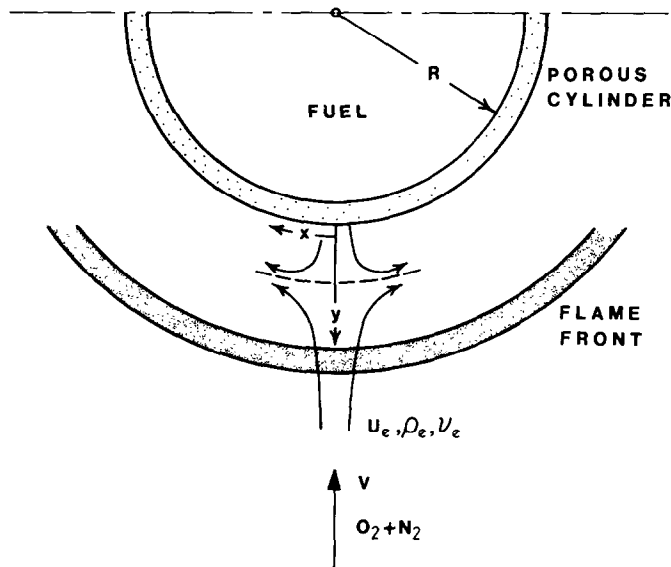


FIG. 4. Stagnation point diffusion flame.

immediate vicinity of the stagnation streamline is

$$\frac{d}{d\eta} \left( \frac{\rho\mu}{\rho_e\mu_e} f'' \right) + f f'' - f'^2 + \rho_e/\rho = 0 \quad (10)$$

and the transformed equation for the conservation of mixture fraction is

$$\frac{d}{d\eta} \left( \frac{1}{Sc} \frac{\rho\mu}{\rho_e\mu_e} \xi' \right) + f \xi' = 0 \quad (11)$$

where  $Sc = \nu/\mathcal{D}$ .

The transport properties in equations (10) and (11) are retained within the differential for the general, variable property case because they are functions of  $\xi(\eta)$ . The use of the diffusivity,  $\mathcal{D}$ , in the equation for  $\xi$  must be clarified. Mixture fractions are based on carbon atom mass fractions in these calculations. However, fuel atoms are incorporated into many different molecules as the original fuel is consumed. Each molecule has a different effective diffusivity [21] in the mixture and a unique diffusivity cannot be ascribed to the fuel atom mass fraction. The approach adopted here is to ascribe to  $\mathcal{D}$  the value of the effective binary diffusivity of nitrogen in the mixture whose composition and temperature are determined by the local value of  $\xi$ . The use of the diffusivity of nitrogen is consistent with the definition of mixture fraction which indicates the equivalence of  $\xi_C$  and  $\xi_N$  if all species diffusivities are equal, i.e.

$$\xi = \frac{Y_C}{Y_{C_0}} = 1 - \frac{Y_N}{Y_{N_\infty}} \quad (12)$$

Subscripts 0 and  $\infty$  refer to mass fractions in the fuel supply and in the approach flow, respectively. In this flame the nitrogen atom and nitrogen molecule mass fractions are equal. As discussed previously,  $\xi_C$  yields a

more accurate representation of the experimental mixture fraction around stoichiometric than  $\xi_N$  or  $\xi_0$  and for that reason it has been used in the present calculations.

Boundary conditions are required to complete the specification of the problem. At the surface of the cylinder  $\eta = 0$  and

$$f_w = f(0) = -(\rho_w/\rho_e)v_w/\sqrt{av_e}. \quad (13)$$

At the cylinder surface the boundary condition for  $\xi$  is

$$\xi(0) = 1 - \rho_w^2/\rho_e^2 \xi_w'/(Sc f_w). \quad (14)$$

Outside the boundary layer the boundary conditions are

$$f(\infty) = 1 \quad (15)$$

and

$$\xi(\infty) = 0. \quad (16)$$

The empirical correlations of  $\xi$  with temperature and composition in the laminar diffusion flame of Tsuji and Yamaoka [18] were used to estimate the transport properties,  $\mu$  and  $\mathcal{D}$ . Wilke's semi-empirical formula [21] provides accurate estimates of the viscosity of a mixture but was found to give values which differed little from a simple mole-weighted average. As a result the mixture viscosity was estimated as being

$$\mu(\xi) = \sum_{i=1}^M X_i(\xi)\mu_i(\xi) \quad (17)$$

with the temperature of the mixture prescribed by  $\xi$ . The effective binary diffusivity of nitrogen in the mixture prevailing at a certain value of  $\xi$  was estimated from the binary diffusivity of nitrogen in each of the component gases. Lenard-Jones potentials were used

to estimate the individual diffusivities [21] and they were combined to yield the effective binary diffusivity so that

$$\mathcal{D}_{N_2} = (1 - X_{N_2}) \bigg/ \sum_{i=1}^{M-1} \frac{X_i}{\mathcal{D}_{N_2,i}}. \tag{18}$$

No account has been taken of thermal (Soret) diffusion which could be significant for lighter species such as  $H_2$  in regions of high temperature gradients near the flame.

Solution of the two coupled equations (10) and (11) was obtained numerically. The equations were written in central-difference forms. The resulting tri-diagonal system of equations was solved iteratively with a Gauss elimination procedure. Cubic spline interpolation was used to evaluate density, viscosity and diffusivity from tabulated values of these properties as functions of the mixture fraction.

RESULTS

Calculations have been performed for a methane–air counterflow diffusion flame for the nominal conditions reported by Tsuji and Yamaoka [18] in their experiments. The non-dimensional fuel ejection rate is  $f_w = -1.5$  and the velocity gradient  $a = 100\text{ s}^{-1}$ . In fact, with the normalization used in equation (9) the corresponding value of  $f_w$  is estimated to be about  $-2$ .

In addition, inspection of the experimental data [18] reveals that the velocity gradient,  $a$ , near the flame front tends towards a value of around  $130\text{ s}^{-1}$ . The calculations have been repeated with these values and the effect on the flame structure is discussed below.

With both  $\rho\mu$  and  $Sc$  as variables the finite-difference calculation of  $\xi$  through the boundary layer for the conditions of Tsuji and Yamaoka [18] shows reasonable agreement (Fig. 5) with the profile of  $\xi_c$  which was derived from the experimental data [18]. The calculated location of the reaction zone at  $\xi = 0.055$  is about 0.4 mm to the air side of the actual flame. The slightly greater thickness of the calculated mixing layer is evident in the temperature profiles which are also presented in Fig. 5. The calculated temperatures are derived simply from the empirical  $\xi_c$ –temperature correlation.

The normal velocity profile is shown in Fig. 6. The calculated stagnation point of the flow coincides with the measured stagnation point at about 1.8 mm from the burner. The calculated maximum velocity agrees well with the measured maximum. The small differences in the locations of temperature and velocity maxima indicate the spatial accuracies of both the experimental method and the numerical scheme.

When the calculations are repeated for  $f_w = -2$  and  $a = 130\text{ s}^{-1}$  the predicted stagnation point of the flow is

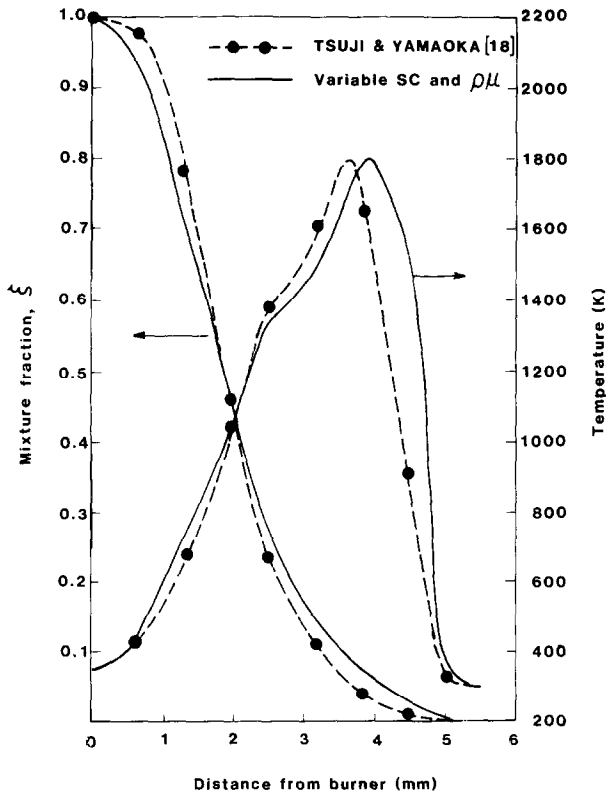


FIG. 5. Calculated profiles of  $\xi$  and temperature with variable properties compared with experimental results.

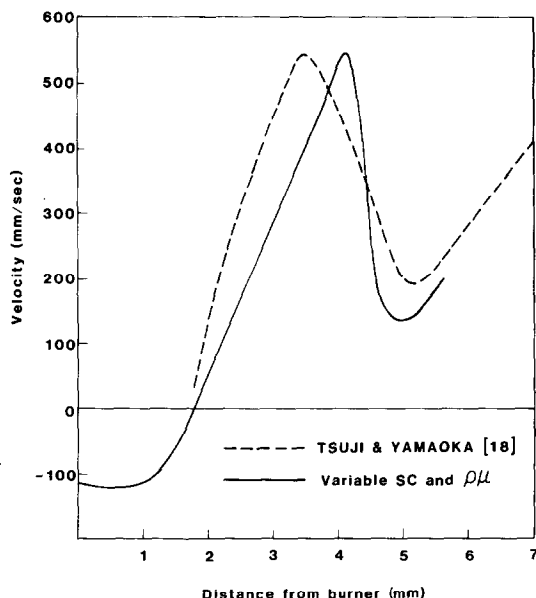


FIG. 6. Calculated normal velocity ( $v$ ) profile with variable properties compared to experimental results.

shifted  $300\text{ }\mu\text{m}$  to the airside of the previously predicted location, i.e. away from the burner. A similar shift in the location of the point of maximum temperature is produced. Near the burner the prediction of mixture fraction is improved compared to the previous calculation but the predicted values of  $\xi$  in the region between 2 to 4 mm from the burner are about 20% larger than the experimental results. The gradient of  $\xi$  at the flame front is increased due to the greater velocity gradient of  $130\text{ s}^{-1}$ . Consequently, the reaction zone is predicted to be thinner with these modified conditions.

Common assumptions in the analysis of reacting boundary layers [7–10] are that the Schmidt numbers are unity and  $\rho_e\mu_e/\rho\mu$  is unity throughout the flow. The profile of  $\xi$  which is obtained from calculations based on these assumptions is compared with the experimental results [18] in Fig. 7 for the same nominal conditions. Deterioration in the agreement between calculation and experiment is evident after comparison with the results obtained with a variable property calculation (Fig. 5); the computed flame position is shifted further to the air side of the actual flame location. The ratio between the calculated distance of the flame from the cylinder and the actual distance is about 1.3. This value can be compared with the results of Takeno [12] who undertook a finite-difference calculation for a methane–air stagnation point diffusion flame with the same configuration and conditions. He assumed that the Schmidt and Lewis numbers for all species were unity and that the ratio  $\rho_e\mu_e/\rho\mu$  was unity throughout the flow. He used a one-step, irreversible reaction (fuel + oxidizer yield product) to determine the reaction rate terms in the conservation equations of species and energy. With these

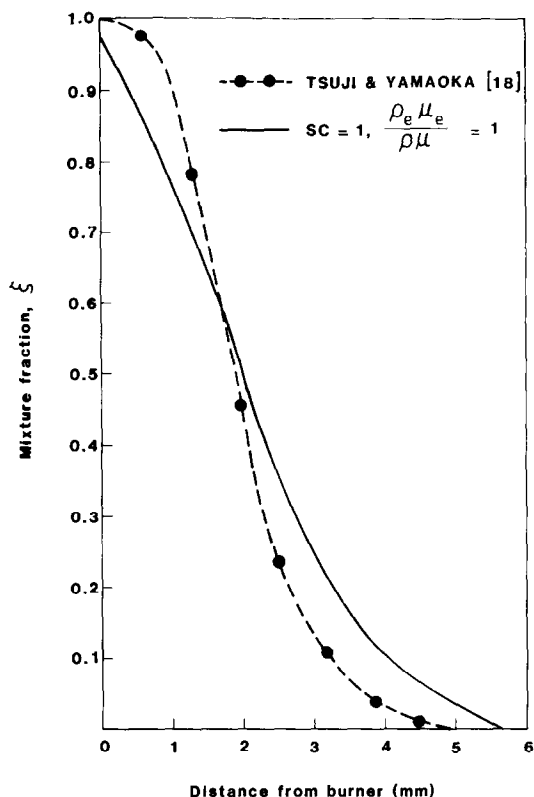


FIG. 7. Calculated profile of  $\xi$  with  $Sc = 1$  and  $\rho_e\mu_e/\rho\mu = 1$  compared with experimental results.

assumptions his calculations resulted in an excessively thick boundary layer with the ratio between his computed flame stand-off distance to the actual measured distance of 1.37. This ratio is similar to the present result.

In order to ascertain the separate influence of each assumption (unit Schmidt number and  $\rho_e\mu_e/\rho\mu$  of unity) the flow was recalculated with, firstly, a unit Schmidt number with variable  $\rho_e\mu_e/\rho\mu$  and, secondly, with a variable Schmidt number and a constant ratio  $\rho_e\mu_e/\rho\mu$ . Figure 8 presents the  $\xi$  profile obtained in the first case. The use of a constant Schmidt number of unity improves the agreement between the calculated  $\xi$  profile and that obtained from the measurements, particularly in the region of the flame reaction zone. This result suggests that the use of a variable Schmidt number in these calculations is not necessary in order to achieve reasonable agreement with measurements, provided that  $\rho\mu$  is variable. The successful use of a unit Schmidt number for the mixture fraction demonstrates that the difficulty inherent in attempting to ascribe a diffusivity to  $\xi$  need not be resolved in a sophisticated manner; an appropriate constant value is satisfactory.

In the second set of calculations a variable Schmidt number was used along with constant values of  $\rho_e\mu_e/\rho\mu$  of 1 and 2. The results of using these approximations are compared with the experimental data in Fig. 9. A constant value for  $\rho_e\mu_e/\rho\mu$  of 1 produces poor

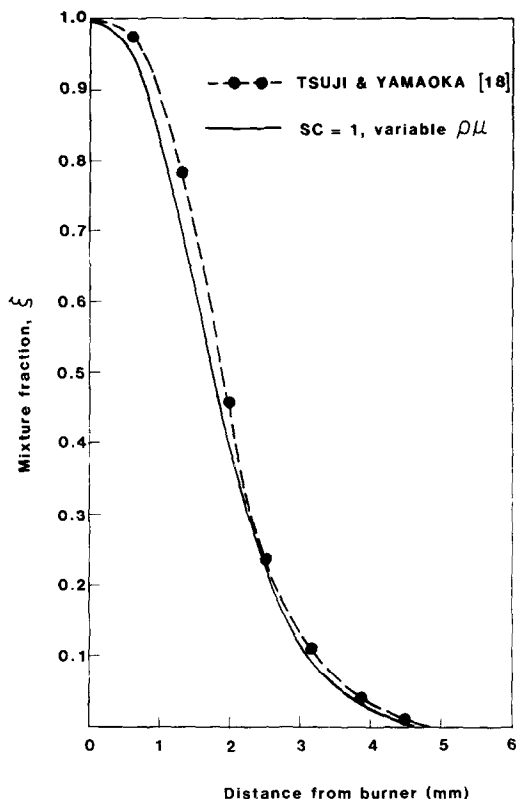


FIG. 8. Calculated profile of  $\zeta$  with  $Sc = 1$  and  $\rho\mu$  variable compared with experimental results.

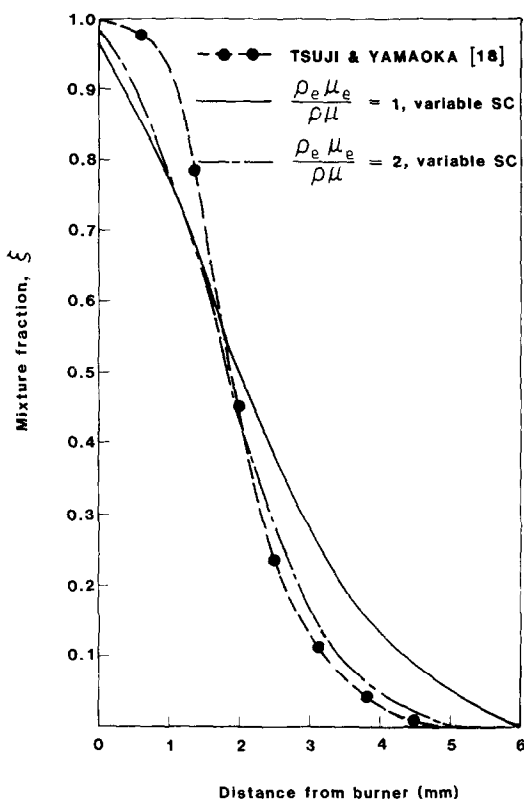


FIG. 9. Calculated profile of  $\zeta$  with variable Schmidt number and constant  $\rho\mu$  compared with experimental results.

agreement with the experimental curve. Setting  $\rho_e\mu_e/\rho\mu$  equal to an average value through the mixing layer of 2 results in much better agreement with the experimental curve except in the region near the burner. Variable values of  $\rho_e\mu_e/\rho\mu$  in the calculation (Fig. 5) achieve better results in this region because  $\rho_e\mu_e/\rho\mu$  reaches its largest value of about 3 close to the burner surface.

A comparison of Fig. 9 (variable Schmidt number and fixed  $\rho_e\mu_e/\rho\mu = 1$ ) with Fig. 7 ( $Sc = 1$  and  $\rho_e\mu_e/\rho\mu = 1$ ) indicates that the error introduced into the prediction of the mixture fractions through the use of the latter set of assumptions can be attributed to variations in  $\rho\mu$ . Figure 8 shows that assuming a unit Schmidt number with variable  $\rho\mu$  actually improves the prediction. The role of variations in  $\rho\mu$  has been advanced by Takeno [12] as the reason for his prediction of an excessively thick boundary layer. The present results support that contention. The dominant effect of  $\rho\mu$  is not unexpected given the factor of 3 variation in its magnitude compared with only 25% variation in the Schmidt number.

Recalculation of the flow for conditions of  $f_w = -2$  and  $a = 130 \text{ s}^{-1}$  indicates that the effect of setting  $Sc$  and  $\rho\mu$  to unity is unchanged in this case. The predicted profile of  $\zeta$  for these conditions is similar to the profile presented in Fig. 7 but it is shifted about  $300 \mu\text{m}$  away from the burner. As a result, the increase in the boundary-layer thickness due to the constant property

assumption is similar to the computed increase obtained for the flow conditions of reference [18]. The modification of the flow conditions does not alter significantly the response of the mixing layer to variations in fluid properties.

## CONCLUSIONS

Transport properties appear in the analysis of a laminar boundary-layer diffusion flame through Schmidt and Lewis numbers in species and energy equations and through the term,  $\rho\mu$ , in the momentum equation. In contrast to the usual modelling assumptions of unit Schmidt and Lewis numbers and  $\rho_e\mu_e/\rho\mu = 1$ , these terms may exhibit significant variations in a diffusion flame. The extent of the variation depends on the fuel. For instance, a methane-air diffusion flame exhibits a factor of 3 variation in  $\rho\mu$  but the variation in a propane-air diffusion flame is less than a factor of 2.

Computer calculations of the mixing within a methane-air diffusion flame have been used to investigate the influence of variable properties in the analysis of a reacting boundary layer. In order to divorce the variable property problem from the coupled chemical kinetics, mixing of fuel and air has been treated in terms of a conserved scalar quantity, the mixture fraction. The temperature and species



concentrations are taken to be functions of the mixture fraction and an empirical correlation of mixture fraction with these thermochemical quantities is used in the calculations.

With a variable Schmidt number and variable  $\rho\mu$ , a finite-difference calculation yielded a profile of mixture fraction which reproduced with reasonable accuracy the profile derived from experimental data. However, the use of the assumptions of unit Schmidt number and  $\rho_e\mu_e/\rho\mu = 1$  resulted in a significantly poorer prediction. Variations in the viscosity term,  $\rho\mu$ , were the dominant influence on the boundary-layer calculations. An average value of  $\rho_e\mu_e/\rho\mu$  through the mixing layer yielded improved results over the assumption of a value of unity.

The effect of variations in  $\rho\mu$  on mixing in the reacting boundary layer was specific to a methane-air diffusion flame; the variations were primarily a result of the low density of methane compared with air. A diminished effect would be expected for a propane-air flame. Nevertheless, it is more appropriate in the analysis of a laminar reacting boundary layer to adopt an average value of  $\rho\mu$  for a specific combination of reactants than to assume that  $\rho_e\mu_e/\rho\mu = 1$ .

## REFERENCES

1. W. M. Kays, *Convective Heat and Mass Transfer*. McGraw-Hill, New York (1966).
2. E. L. Knuth, Use of reference states and constant property solutions in predicting mass, momentum and energy transfer rates in high-speed laminar flows, *Int. J. Heat Mass Transfer* **6**, 1–22 (1963).
3. G. L. Hubbard, V. E. Denny and A. F. Mills, Droplet evaporation: effects of transients and variable properties, *Int. J. Heat Mass Transfer* **18**, 1003–1008 (1975).
4. C. K. Law and F. A. Williams, Kinetics and convection in the combustion of alkane droplets, *Combust. Flame* **19**, 393–405 (1972).
5. R. Srivastava and D. E. Rosner, A new approach to the correlation of boundary layer mass transfer rates with thermal diffusion and/or variable properties, *Int. J. Heat Mass Transfer* **22**, 1281–1294 (1979).
6. F. A. Williams, *Combustion Theory*. Addison-Wesley, Reading, Mass. (1965).
7. P. M. Chung, F. E. Fendell and J. F. Holt, Nonequilibrium anomalies in the development of diffusion flames, *AIAA J* **4**, 1020–1026 (1966).
8. T. Saitoh, Extinction analysis of premixed flame for counter flow and blunt body forward stagnation region flow, *Int. J. Heat Mass Transfer* **17**, 1063–1077 (1974).
9. T. Saitoh, An investigation of the diffusion flame around a porous cylinder under conditions of natural convection, *Combust. Flame* **36**, 233–244 (1979).
10. P. A. Libby and F. A. Williams, Structure of laminar flamelets in premixed turbulent flames, *Combust. Flame* **44**, 287–303 (1982).
11. A. G. Marathe and V. K. Jain, Some studies on opposed-jet diffusion flame considering general Lewis numbers, *Combust. Sci. Tech.* **6**, 151–157 (1972).
12. T. Takeno, A gas dynamic analysis of a counter-flow diffusion flame, *Combust. Sci. Tech.* **5**, 99–106 (1972).
13. S. Ishizuka and H. Tsuji, Effects of transport properties and flow non-uniformity on the temperature of counterflow diffusion flames, *Combust. Sci. Tech.* **37**, 171–191 (1984).
14. N. Peters, Analysis of a laminar flat plate boundary layer diffusion flame, *Int. J. Heat Mass Transfer* **19**, 385–393 (1976).
15. G. Dixon-Lewis, S. Fukutani, J. A. Miller, N. Peters and J. Warnatz, Calculation of the structure and extinction limit of a methane-air counterflow diffusion flame in the forward stagnation region of a porous cylinder, *20th Symposium (Int.) on Combustion*, Combustion Institute, to be published.
16. R. W. Bilger, Reaction rates in diffusion flames, *Combust. Flame* **30**, 277–284 (1977).
17. R. E. Mitchell, A. F. Sarofim and L. A. Clomburg, Experimental and numerical investigation of confined laminar diffusion flames, *Combust. Flame* **37**, 227–244 (1980).
18. H. Tsuji and I. Yamaoka, Structure analysis of counterflow diffusion flames in the forward stagnation region of a porous cylinder, *13th Symposium (Int.) on Combustion*, pp. 723–731, Combustion Institute (1971).
19. J. A. Miller, R. J. Kee, M. D. Smooke and J. F. Grcar, The computation of the structure and extinction limit of a methane-air stagnation point diffusion flame, Paper WSS/CI 84-10 presented at 1984 Spring Meeting of the Western States Section, Combustion Institute, University of Colorado, Boulder (April 1984).
20. S. I. Abdel-Khalik, An investigation of the diffusion flame surrounding a simulated fuel droplet. Ph.D. thesis, University of Wisconsin, Madison (1973).
21. R. B. Bird, W. E. Stewart and E. N. Lightfoot, *Transport Phenomena*. Wiley, New York (1960).
22. H. Tsuji and I. Yamaoka, The structure of counterflow diffusion flames in the forward stagnation region of a porous cylinder, *12th Symposium (Int.) on Combustion*, pp. 997–1005, The Combustion Institute (1969).
23. P. M. Chung, Chemically reacting nonequilibrium boundary layers. In *Advances in Heat Transfer*, Vol. 2. Academic Press, New York (1965).

## EFFETS DES PROPRIETES VARIABLES DANS L'ANALYSE DU POINT D'ARRET D'UNE FLAMME DE DIFFUSION

**Résumé**—On étudie numériquement l'effet des variations des propriétés du fluide sur l'analyse du point d'arrêt d'une flamme de diffusion. La thermochimie de la flamme est décrite par une formulation empirique des concentrations des espèces et de la température avec un scalaire conservé (la fraction massique d'atomes de combustible). De cette façon, le mécanisme de mélange dans la flamme de diffusion est découplée de la cinétique chimique. La variation du nombre de Schmidt pour la fraction de mélange n'a pas un effet significatif sur la prévision numérique du profil de fraction de masse atomique dans la flamme. Néanmoins, l'hypothèse d'une valeur constante de  $\rho\mu$  à travers la flamme méthane-air cause une surestimation significative de l'épaisseur de la couche de mélange. Une valeur moyenne de  $\rho\mu$  à travers la couche limite donne une estimation satisfaisante du profil de fraction de masse.

# DER EINFLUSS VERÄNDERLICHER STOFFEIGENSCHAFTEN BEI DER UNTERSUCHUNG EINER STAUPUNKTS-DIFFUSIONSFLAMME

**Zusammenfassung**—Der Einfluß von Stoffeigenschaftsänderungen auf eine Staupunkts-Diffusionsflamme wurde numerisch untersucht. Die Thermochemie der Flamme wurde über einen empirischen Zusammenhang ermittelt, wobei die Konzentration der Komponenten und die Temperatur vom Atommassenanteil des Brennstoffes abhängen. Dadurch konnte der Mischungsvorgang in der Diffusionsflamme unabhängig von der chemischen Kinetik untersucht werden. Der Einfluß veränderlicher Schmidt-Zahlen ist bei der numerischen Bestimmung der Atommassenverteilung gering. Die Annahme eines konstanten Wertes für  $\rho \cdot \mu$  in der Methan-Luft-Flamme verursacht jedoch, daß die Mischungsschichtdicke um einiges zu groß berechnet wird. Mit einem über die Grenzschicht gemittelten Wert für  $\rho \cdot \mu$  ist es möglich, das Profil der Massenverteilung zufriedenstellend zu berechnen.

## ЭФФЕКТЫ ИЗМЕНЕНИЯ СВОЙСТВ ПРИ АНАЛИЗЕ ДИФFUЗНОГО ПЛАМЕНИ В ТОЧКЕ ТОРМОЖЕНИЯ

**Аннотация**—Влияние изменения свойств жидкости на анализ диффузного пламени в точке торможения рассчитывается численно. Термохимия пламени задается эмпирической зависимостью концентраций и температур образцов с сохраненным скаляром (массовой доли атомов топлива). Таким образом, процесс смешения в диффузном пламени был отделен от химической кинетики. Изменения числа Шмидта для доли смеси не оказывали существенного влияния на численные расчеты профиля массовой доли атома в пламени. Однако, предположение о постоянном значении  $\rho \mu$  для метано-воздушной смеси приводит к значительному перерасчету толщины слоя смешения. Среднее значение  $\rho \mu$  по всему пограничному слою дает удовлетворительные расчеты профиля массовой доли.